JPEDAV (2005) 26:215-224
DOI: 10.1361/15477030523715
1547-7037/$19.00 ©ASM International

Correlation and Prediction of Interface Tension for Fluid Mixtures: An Approach Based on Cubic Equations of State with the Wong-Sandler Mixing Rule

Andrés Mejía, Hugo Segura, Jaime Wisniak, and Ilya Polishuk

(Submitted June 4, 2004; in revised form January 24, 2005)

Concentration profiles, interface thickness, and interface tensions have been calculated for mixtures applying the gradient theory to the Peng-Robinson equation of state. The approach is based on an accurate local fit of vapor-liquid equilibrium (VLE) data, and, for this purpose, the flexibility of the original Wong-Sandler mixing rule has been taken into account. Correlation and prediction capabilities of experimental interfacial tension data are analyzed for the quadratic mixing rule and the present approach. The method, which is discussed in detail in this work, provides an improved scheme for calculating interfacial properties, both for polar and nonpolar mixtures. According to results, a better correlation and prediction of the interfacial tensions can be obtained from an adequate interpolation of the VLE, using simple cubic equations of state. Examples are presented for binary and ternary mixtures.

1. Introduction

The interfacial tension (σ) between phases is an important physical property because many physical and chemical processes take place at the interface of solids, liquids, and vapors. Typical cases in which the interfacial behavior plays a central role are the adhesion of surfaces, stability of foams, generation of drops and bubbles, wetting, coating, recovery of oil from wells, and phase behavior in porous media.[1] These processes differ considerably from those observed in the corresponding bulk phase and depend drastically on the magnitude of σ.

Due to its technological importance, a theoretical approach that is able to correlate or predict σ as a function of temperature, pressure, and concentration is valuable from a practical viewpoint. One of the most successful approaches is the gradient theory (GT), originally developed by van der Waals, and reformulated later by Cahn and Hilliard.[2] Briefly, the GT describes a continuous evolution of the density of the Helmholtz energy along the interface, from which the interfacial concentration profile and σ can be calculated. Since then, many works have been devoted to improve the results of the GT by modeling the Helmholtz energy with different equations of state (EOS). A significant advantage of such an approach is that a common EOS model can be used to calculate σ and the phase equilibrium condition that promotes the coexistence of phases.

As follows from the recent review of Kahl and Enders,[3] major work regarding the prediction of σ has been based on standard cubic EOSs with using a quadratic mixing rule (QMR). Such a combination yields adequate predictions for simple mixtures, like the type I systems in the classification of van Konynenburg and Scott.[4] For example, Carey and colleagues[5,6] and Cornelisse and colleagues[7-9] have predicted σ for hydrocarbon mixtures using the Peng-Robinson EOS (PR-EOS).[10] Carey and colleagues,[5,6] Cornelisse and colleagues,[7-9] Sahimi and Taylor,[11] and Miqueu et al.[12] have demonstrated that GT with PR-EOS and QMR also brings excellent results in calculating σ in binary and ternary mixtures of carbon dioxide with hydrocarbons. However, for the case of standard cubic EOSs, the prediction of the interfacial behavior for polar mixtures may be inaccurate or, even, nonphysical.[7] These limitations follow from the fact that the QMR has a limited capability for interpolating the vapor-liquid equilibrium (VLE) of polar systems.[13]

The limitation of the GT in predicting σ of polar mixtures may be overcome by using different approaches. One possibility is to consider an EOS that is able to treat complex mixtures. For example, good results have been reported for the APACT model (Associated Perturbed Anisotropic Chain) by Cornelisse and colleagues[6,14] and for the SAFT model (Statistical Associating Fluid Theory) by Kahl and Enders.[15] An alternative approach is to consider a cubic EOS of the van der Waals type with improved mixing rules. The latter approach is well established for treating VLE problems in engineering practice,[13] although its capability for predicting σ has not yet been analyzed.

In this work, we explore the prediction capability of the GT applied to the PR-EOS, appropriately modified for fitting vapor pressures of pure components, together with the mixing rule proposed by the Wong and Sandler (WS).[16] Our approach is exemplified with binary mixtures of alcohols plus water in the low-pressure range, and with a ternary mixture of carbon dioxide plus hydrocarbons in the high-pressure range.

Andrés Mejía and **Hugo Segura,** Departamento de Ingeniería Química, Universidad de Concepción, P.O. Box 160-C-Correo 3, Concepción, Chile; **Jaime Wisniak,** Department of Chemical Engineering, Ben-Gurion University of the Negev, Beer-Sheva 84105, Israel; and **Ilya Polishuk,** the Department of Chemical Engineering and Biotechnology, the College of Judea and Samaria, Ariel, Israel. Contact e-mail: amejia@diq.udec.cl.

2. Theory

2.1 Gradient Theory

According to the GT, the interfacial fluid between bulk phases in equilibrium obeys the condition of minimum energy. For a planar vapor-liquid interface, this condition is given by a set of partial differential equations that describes the dependence of the concentration of each component along the interface length z.[5-9,11,12] Expressed in terms of concentrations, the fundamental equation of the GT is:

$$\left[\sum_{i,j=1}^{n_c} c_{ij}\left(\frac{d\rho_i}{d\rho_s}\right)\left(\frac{d\rho_j}{d\rho_s}\right)\right]\left[H_s\frac{d\rho_k}{d\rho_s}-H_k\right] + 2(\Phi+P^0)|C|\left(\frac{d^2\rho_k}{d\rho_s^2}\right)=0 \quad \text{(Eq 1)}$$

$k = 1, 2, \ldots, s-1, s+1, \ldots, n_c$

where n_c stands for the number of components, c_{ij} is the cross-influence parameter ($= c_{ji}$), ρ_i is the concentration of component i (related to the concentration of the mixture ρ by $\rho_i = x_i \rho$), and P^0 is the bulk equilbrium pressure. H_k is the kth component of the vector function $\boldsymbol{H}$ given by:

$$\mathbf{H}(\rho) = |\boldsymbol{C}|\boldsymbol{C}^{-1}\nabla_\rho^T(\Phi+P^0) \quad \text{(Eq 2)}$$

$|\boldsymbol{C}|$ is the determinant of the influence parameter matrix $\boldsymbol{C}$ defined as:

$$\boldsymbol{C}=\begin{bmatrix} c_{11} & \cdots & c_{1n_c} \\ \vdots & \ddots & \vdots \\ c_{n_c1} & \cdots & c_{n_cn_c}\end{bmatrix} \quad \text{(Eq 3)}$$

and ∇_ρ is the following vector operator

$$\nabla_\rho=\left[\frac{\partial}{\partial\rho_1}\cdots\frac{\partial}{\partial\rho_{n_c}}\right]^T \quad \text{(Eq 4)}$$

Finally, in Eq 1 and 2, Φ correspondes to the grand thermodynamic potential defined as:

$$\Phi[\rho_i(z),\rho(z)] = a_0[\rho_i(z),\rho(z)] - \sum_{i=1}^{n_c}\rho_i(z)\mu_i^0[T^0,V^0,\rho_i^0] \quad \text{(Eq 5)}$$

In Eq 5, a_0 is the density of the Helmholtz energy of the homogeneous system (i.e., the bulk phase), μ_i^0 is the chemical potential of component i at equilibrium and, V^0, T^0, ρ_i^0 are the equilibrium volume, temperature, and concentration of component i, respectively. a_0 and μ_i^0 can be directly determined from an EOS using the following expressions[17,18]:

$$\frac{a_0}{\rho RT}=\int_0^\rho\left(\frac{P}{RT\rho^2}-\frac{1}{\rho}\right)d\rho+\frac{1}{\rho}\sum_{i=1}^{n_c}\rho_i\ln\rho_i \quad \text{(Eq 6a)}$$

$$\mu_i^0=\left(\frac{\partial a_0}{\partial\rho_i}\right)_{T^0,V^0\rho_{j\neq i}^0} \quad \text{(Eq 6b)}$$

Nomenclature

a	cohesion parameter in the PR-EOS
a_0	Helmholtz energy density of the homogeneous system
b	covolume parameter in the PR-EOS
c_{ii}	influence parameter of pure component i
c_{ij}	cross influence parameter
$\boldsymbol{C}$	matrix of the influence parameters
g_{nx}	n-esima derivative of Gibbs energy with respect to x (see Eq. 14)
G	Gibbs energy
$\boldsymbol{H}$	auxiliary vector
H_k	kth component of the auxiliary vector $\boldsymbol{H}$
k	interaction parameter for the mixing rule
m	parameter of the thermal cohesive function of PR-EOS (Soave's factor)
n_c	number of components
P	absolute pressure
R	universal gas constant
SP	stationary point
T	absolute temperature
V	volume
x, y	mole fractions of the liquid and vapor phases
z	normal distance to the interface

Greek

α_i	thermal cohesive function of the species i
α	NRTL parameter
χ	adjustable parameter
Φ	grand thermodynamic potential
σ	interfacial tension
μ	chemical potential
ρ	molar concentration
ρ_s	molar concentration used as integration variable
τ	NRTL parameter
Λ	Wilson parameter

Subscripts

c	critical
exp	experimental
i, j, l, k	species
s	independent variable

Superscripts

L	liquid
V	vapor
0	equilibrium

In Eq 6, R is the gas constant, T is temperature, and P is pressure. According to the GT, σ can be calculated by solving[5-9,11,12]:

$$\sigma = \int_{\rho_s^V}^{\rho_s^L} \left[2(\Phi + P^0) \sum_{i,j=1}^{n_c} c_{ij} \left(\frac{d\rho_i}{d\rho_s} \right) \left(\frac{d\rho_j}{d\rho_s} \right) \right]^{1/2} d\rho_s \qquad \text{(Eq 7)}$$

The integration of Eq 7 requires the solution of Eq 1, which provides the topology of the concentration profiles ρ_i along the interface, from bulk to bulk phase. Inspection of Eq 1 to 7 reveals that the calculation of σ depends on c_{ij}, the EOS model and its mixing rules.

In this work, c_{ij} is calculated using the procedure suggested by Carey and colleagues[5,6] and Cornelisse and colleagues.[7-9] For the case of pure fluids ($i = j$), c_{ii} is calculated at a constant temperature from experimental σ values (σ_{exp}) as:

$$c_{ii}(T^0) = \sigma_{exp}^2(T^0) \left(\int_{\rho^{0,V}}^{\rho^{0,L}} \sqrt{2(\Phi + P^0)}\, d\rho_i \right)^{-2} \qquad \text{(Eq 8)}$$

and its temperature dependence is correlated by a linear function. For the case of mixtures ($i \neq j$), c_{ij} is obtained by averaging the pure component influence parameters according to:

$$c_{ij} = (1 - \chi_{ij})\sqrt{c_{ii}c_{jj}} \qquad \chi_{ij} = \begin{cases} 0 & \text{if } i = j \\ \chi_{ji} & \text{if } i \neq j \end{cases} \qquad \text{(Eq 9)}$$

where χ_{ij} is a symmetric adjustable parameter that, in turn, may be obtained from the fit of experimental σ data of mixtures. Due to stability requirements χ_{ij} should be bounded to the range $0 \leq \chi_{ij} < 1$.[5,7,19,20] When χ_{ij} is zero, the set of differential equations indicated in Eq 1 becomes the following set of algebraic equations[5,7,11,12]:

$$\sqrt{c_{ss}}[\mu_k(\rho) - \mu_k^0] = \sqrt{c_{kk}}[\mu_s(\rho) - \mu_s^0]$$
$$k = 1, 2, \ldots, s-1, s+1, \ldots, n_c \qquad \text{(Eq 10)}$$

As we stated before, besides c_{ij}, the calculation of σ depends on the EOS model and its mixing rules through the chemical potential. In this work, the chemical potential of phases and interfaces has been represented by the PR-EOS. In addition, the QMR and the original WS mixing rules have been considered for correlating experimental VLE data and to predict ($\chi_{ij} = 0$) or to correlate ($\chi_{ij} \neq 0$) σ in mixtures. Due to several modifications that have been proposed for the PR-EOS and the mixing rules used in this work in the Appendix, we summarized, briefly, the main expressions used for the homogeneous fluids (e.g., PR-EOS, as well as the QMR and the original WS mixing rules).

2.2 Gradient Theory Projections

As in the molecular-dynamics approach,[22,23] the GT yields a rich description of properties along the interface. These results may be collected in the following set of projections, which are useful to analyze the interface behavior and its relation to some VLE features:

2.2.1 ρ_i–ρ_j Projection. This projection is generated by solving Eq 1 or Eq 10. From this diagram, it is possible to quantify the population of species at the interface and the surface activity of a mixture (or molar accumulation of the species at the interfaces). The surface activity is characterized by the condition $(d\rho_i/d\rho_j) = 0$, which states the existence of stationary points (SPs) of concentration along the interface.

2.2.2 z–ρ_i Projection. This projection is useful in describing the concentration of species along the interface length and may be directly compared to molecular-dynamics predictions.[24,25] The z–ρ_i diagram may be obtained from the ρ_j–ρ_i projection using the following relations:

$$\left(\frac{d\rho_s}{dz} \right)^2 = \frac{2\Delta\Phi}{\sum_{i,j=1}^{n_c} c_{ij} \left(\frac{d\rho_i}{d\rho_s} \right) \left(\frac{d\rho_j}{\rho_s} \right)} \qquad \text{for } k = s \qquad \text{(Eq 11a)}$$

$$\frac{d\rho_k}{dz} = \left(\frac{d\rho_k}{d\rho_s} \right) \left(\frac{d\rho_s}{dz} \right) \qquad \text{for } k = 1, 2, \ldots, s-1, s+1, \ldots, n_c \qquad \text{(Eq 11b)}$$

where

$$\Delta\Phi = \Phi + P^0 \qquad \text{(Eq 12)}$$

From Eq 11, it is possible to conclude that the SPs are also reflected in the z–ρ_i projection as points at which $(d\rho_i/dz) = 0$.

2.2.3 ρ_i–ΔΦ Projection. This projection is related to the ρ_j–ρ_i projection by Eq 5 and 12. In this case, SPs are reflected by the condition $(\partial\Delta\Phi/\partial\rho_i) = \infty$. It is interesting to observe that this projection also involves equilibrium information, as follows from the relations:

$$\left(\frac{\partial\Delta\Phi}{\partial\rho_i} \right)_{T^0, V^0, \rho_{j\neq i}^0} = \mu_i - \mu_i^0 = 0 \qquad \text{(Eq13a)}$$

$$\left(\frac{\partial^2\Delta\Phi}{\partial\rho_i^2} \right)_{T^0, V^0, \rho_{j\neq i}^0} = \left(\frac{\partial\mu_i}{\partial\rho_i} \right)_{T^0, V^0, \rho_{j\neq i}^0} > 0 \qquad \text{(Eq 13b)}$$

Equation 13a is equivalent to the necessary VLE condition at constant temperature. In addition, Eq 13b is a differential stability condition for interfaces that are comparable to the Gibbs energy (G) stability constraint of a single phase.[26] According to our results, we have observed that the sign constraint of Eq 13b is satisfied in the following two cases:

- The phases involved in an equilibrium state are globally stable; and
- Metastable phase equilibrium states characterized by the condition:

$$\left(\frac{\partial^n G/RT}{\partial x_i^n}\right)_{T,P} = g_{nx} \geq 0 \qquad (n = 2,3) \qquad \text{(Eq 14)}$$

Consequently, the inspection of the minima in $\rho - \Delta\Phi$ establishes whether the VLE is stable (absolute minima of $\Delta\Phi$) or metastable (relative minima of $\Delta\Phi$).[22,27]

2.2.4 x–σ and P–σ Projections. The x–σ diagram is obtained directly from Eq 7, while the P–σ diagram is obtained by combining the x–σ and x–P projections (the latter obtained from VLE calculations). The relation between the x–P and P–σ projections follows from the identity:

$$\left(\frac{\partial P}{\partial x}\right)_T = \left(\frac{\partial P}{\partial \sigma}\right)_T \left(\frac{\partial \sigma}{\partial x}\right)_T \qquad \text{(Eq 15)}$$

which allows establishing that an azeotropic point in the x–P diagram ($[\partial P/\partial x]_T = 0$), is reflected by the singularity $[\partial\sigma/\partial P]_T = \infty$ in the P–σ projection.

3. Procedure for Calculations

The following sequential steps are suggested for calculating σ.

- Calculate the VLE and characterize the stability of the predicted phases;
- Fit c_{ii}, as described in Eq 8 and fix the value of χ_{ij} within the range $0 \leq \chi_{ij} < 1$;
- Select the variable of integration ρ_s in Eq 1, provided that ρ_s must exhibit a monotonic behavior along the interface region;
- Discretisize ρ_s between the concentration of bulk phases;
- Solve Eq 1 for the concentration of the other components $\rho_1, \ldots, \rho_{s-1}, \rho_{s+1}, \ldots \rho_{nc}$ for each ρ_s. Initial ρ_i values may be taken from the solution of Eq 10;
- Calculate σ from Eq 7; and
- Test other χ_{ij} values to minimize σ deviations.

4. Results

To test the approach described in this work, we have selected a set of binary mixtures of water plus alcohol at 303.15 K in the low-pressure range and a ternary system (carbon dioxide with hydrocarbons) at 344.30 K in the high-pressure range. Table 1 summarizes the physical properties of the pure components. Table 2 presents the mixing rule parameters, and Table 3 contains the temperature, pressure, and concentration ranges of the experimental data that were used to fit the mixing rule parameters shown in Table 2. Finally, Table 4 summarizes deviation statistics for VLE predictions.

As established in section 2, a properly parametrized EOS together with c_{ii} values provide the information required to characterize interfacial behavior. The absolute average deviation overall deviations for σ (AADσ%), as obtained for the mixtures discussed in this work, are presented in Table 4. For these calculations, the optimal χ_{ij} values were 0 for methanol plus water and for the ternary system carbon dioxide plus butane plus decane, 0.1 for ethanol plus water, and 0.15 for propan-1-ol plus water, and propan-2-ol plus water.

Table I Physical properties of the pure components

Fluid	T_c, K	P_c, MPa	m_i	T, K	$10^{20} \times c_{ii}$/J m^5 mol^{-2}
Butane(a)(b)	425.20	3.80	0.6716	344.30	20.3850(i)
Carbon dioxide(a)(c)	304.20	7.38	0.6942	344.30	3.1483(i)
Decane(b)(c)	617.60	2.11	1.0579	344.30	134.0870(i)
Ethanol(d)(h)	516.20	6.38	1.2541	303.15	4.1281
Methanol(e)(h)	512.60	8.10	1.1376	303.15	2.4130
Propan-1-ol(f)(h)	536.70	5.17	1.2780	303.15	8.2608
Propan-2-ol(g)(h)	508.30	4.76	1.3246	303.15	8.9390
Water(d)-(h)	647.30	22.05	0.8438	303.15	1.4061

Note: Critical properties were taken from Reid et al.[30] m_i, parameter of the thermal cohesive function of PR-EOS (Soave's factor),[10] which was fitted from experimental vapor pressure data. Experimental vapor pressure data taken from: (a) Hsu et al.[31]; (b) Raemer and Sage[32]; (c) Nagarajan and Robinson[33]; (d) Pemberton and Mash[34]; (e) McGlashan and Williamson[35]; (f) Udovenko and Mazanko[36]; (g) Udovenko and Mazanko.[37] c_{ii} was fitted from the experimental interfacial tension data and evaluated at T. These experimental data were taken from (a) Hsu et al.[31]; (c) Nagarajan and Robinson[33] and (h) Vázquez et al.[38] (i) The c_{ii} values are in good agreement to those reported by Cornelisse,[7] Cornelisse et al.,[8,9] Sahimi and Taylor,[11] Miqueu et al.,[12] Mejía et al.,[28] and Miqueu.[29]

According to the results in the Table 4, we can conclude that better VLE correlations are reflected by improved σ predictions ($\chi_{ij} = 0$) or σ correlations ($\chi_{ij} \neq 0$). This result is useful for establishing, which mixing rule may be used to calculate VLE and σ simultaneously. From the quoted table, we also observe that the combination GT with PR-EOS and original WS mixing rule permits the calculation of interfacial behavior in mixtures of propanol plus water in which QMR is unable to describe the interfacial behavior due to this mixing rule predicting false immiscibility gaps for these mixtures. Specific details involved in the prediction of σ for each mixture are described below.

4.1 Binary Systems

Concentration profiles (ρ_i–ρ_j) are the basic piece of information needed to calculate σ according to Eq 7. These profiles are shown in Fig. 1 for the methanol plus water mixture at different mole fractions. ρ_1 and ρ_2 were calculated from the original WS mixing rule coupled to Wilson's model (see details in Table 4). From Fig. 1, it is possible to observe that the system exhibits surface activity for the whole mole fraction range (a single SP, *A,* appears for water). Figure 2, in turn, depicts the z–ρ_i projection. In this case, the SPs that appear in Fig. 1 (point A) are reflected in Fig. 2 (point B), as can be expected from the discussion in Section 2.2. It is interesting to note that, as a direct consequence of the SPs, the concentration inside the interface could be locally larger than the concentration in bulk

Table 2 Binary parameters for mixing rules

System	QMR	WS + Wilson			WS + NRTL			
	k_{ij}	k_{ij}	Λ_{ij}	Λ_{ij}	k_{ij}	α_{ij}	τ_{ij}	τ_{ji}
Butane + decane(a)	3.9916×10^{-3}	3.2464×10^{-1}	1.1090	0.7501	3.3820×10^{-1}	0.1219	2.3293	−1.7661
Carbon dioxide + butane(b)	1.2463×10^{-1}(h)	4.1206×10^{-1}	1.0715	0.1995	4.0728×10^{-1}	0.4523	7.1935	0.4789
Carbon dioxide + decane(c)	9.5821×10^{-2}(h)	7.2592×10^{-1}	0.8759	0.0360	6.9503×10^{-1}	0.3866	5.5833	0.4172
Ethanol + water(d)	-1.0846×10^{-1}	2.3257×10^{-1}	0.3666	0.5944	2.3344×10^{-1}	0.4000	0.4376	1.0243
Methanol + water(e)	-8.9457×10^{-2}	8.1962×10^{-2}	0.4103	1.1595	8.3777×10^{-2}	0.4500	−0.1785	0.9075
Propan-1-ol + water(f)	-1.2605×10^{-1}	3.9572×10^{-1}	0.1238	0.3524	3.9039×10^{-1}	0.4000	0.8715	1.9725
Propan-2-ol + water(g)	-1.7771×10^{-1}	3.4723×10^{-1}	0.2013	0.4330	3.4655×10^{-1}	0.4000	0.6280	1.6335

Note: The parameters for the mixing rules were fitted from experimental VLE data taken from the following: (a) Raemer and Sage[32]; (b) Hsu et al.[31]; (c) Nagarajan and Robinson[33]; (d) Pemberton and Mash[34]; (e) McGlashan and Williamson[35]; (f) Udovenko and Mazanko[36]; (g) Udovenko and Mazanko.[37] (h) The k_{ij} values are in good agreement to those reported by Cornelisse,[7] Cornelisse et al.,[8,9] Sahimi and Taylor,[11] Miqueut et al.,[12] Mejía et al.,[28] and Miqueu.[29]

Table 3 Range of temperature, pressure, and concentration of the experimental data used to fit mixing rule parameters

System	Temperature range, K	Pressure range, MPa	Mole fraction range
Butane + decane(a)	310.93-510.93	5×10^{-4}-4.92	0.0-1.0
Carbon dioxide + butane(b)	319.30-377.60	2.18-7.58	0.188-0.873
Carbon dioxide + decane(c)	344.30-377.60	6.38-16.48	0.457-0.925
Ethanol + water(d)	303.15-363.15	4.25×10^{-3}-1.59×10^{-1}	0.0-1.0
Methanol + water(e)	303.15-338.15	5.62×10^{-3}-1.03×10^{-1}	0.0-1.0
Propan-1-ol + water(f)	303.15-333.15	4.28×10^{-3}-3.11×10^{-2}	0.0-1.0
Propan-2-ol + water(g)	303.15-333.15	4.28×10^{-3}-4.26×10^{-2}	0.0-1.0

(a) Raemer and Sage[32]; (b) Hsu et al.[31]; (c) Nagarajan and Robinson[33]; (d) Pemberton and Mash[34]; (e) McGlashan and Williamson[35]; (f) Udovenko and Mazanko[36]; (g) Udovenko and Mazanko.[37]

Table 4 Statistic deviations in vapor pressure and vapor phase mole fractions for vapor-liquid equilibrium correlations and for prediction of interfacial tensions

System	QMR			WS + Wilson			WS + NRTL		
	AADP, %(a)	Δy_1(b)	AADσ, %(a)	AADP, %	Δy_1	AADσ, %	AADP, %	Δy_1	AADσ, %
Carbon dioxide + butane + decane(c)	1.5	2.0	23.1	3.3	1.0	25.4	2.4	1.0	18.5
Ethanol + water(d)	4.9	2.8	6.9	0.8	0.5	3.3	0.7	0.5	2.4
Methanol + water(d)	2.4	1.1	2.6	1.6	0.9	2.4	1.6	0.9	2.4
Propan-1-ol + water(d)	7.0	4.8	NC(e)	1.6	0.9	1.3	1.7	1.2	1.3
Propan-2-ol + water(d)	8.8	6.1	NC	1.3	1.0	2.2	0.9	1.0	1.9

Note: AAD, absolute average deviation; NC, not calculated. VLE deviations are measured with respect to the experimental VLE data referred to in Table 1. (a) $AAD\delta = (100/N_P) \sum_{i=1,NP} |\delta_i^{exp} - \delta_i^{cal}|/\delta_i^{exp}$ (δ = P, or σ). (b) $\Delta y_1 = (100/N_P) \times \sum_{i=1,NP} |y_i^{exp} - y_i^{cal}|$, where N_P is the number of experimental points. (c) σ data were taken from Nagarajan et al.[39] (d) σ data were taken from Vázquez et al.[38] (e) Not calculated because the mixing rule predicts false immiscibility gaps for one of its binaries (carbon dioxide + decane; see Table 2).

phases. The former result agrees well with the discussion of Winkelmann,[23] for mixtures of hydrocarbons, and with the previous results of Cornelisse and colleagues.[7-9]

Finally, Fig. 3 shows the $\rho-\Delta\Phi$ profile for the methanol-plus-water mixture. This profile displays two minima (points C and D) at equilibrium conditions. This behavior confirms that two phases, liquid and vapor, are present at the temperature for which the VLE has been calculated.

It should be pointed out that the $\rho_i-\rho_j$, $\rho-\Delta\Phi$, and $z-\rho_i$ projections are similar for all the binary mixtures considered in this work.

Figures 4 and 5 depict the dependence of σ on P and on x_1. Focusing our attention on these figures, it is possible to conclude that for zeotropic systems (Fig. 4), σ vapor pressure exhibits a negative slope, which indicates that σ decreases as the vapor pressure (or the concentration) increases. For the case of azeotropic systems (i.e., ethanol, propan-1-ol, and propan-2-ol plus water), σ decreases as P

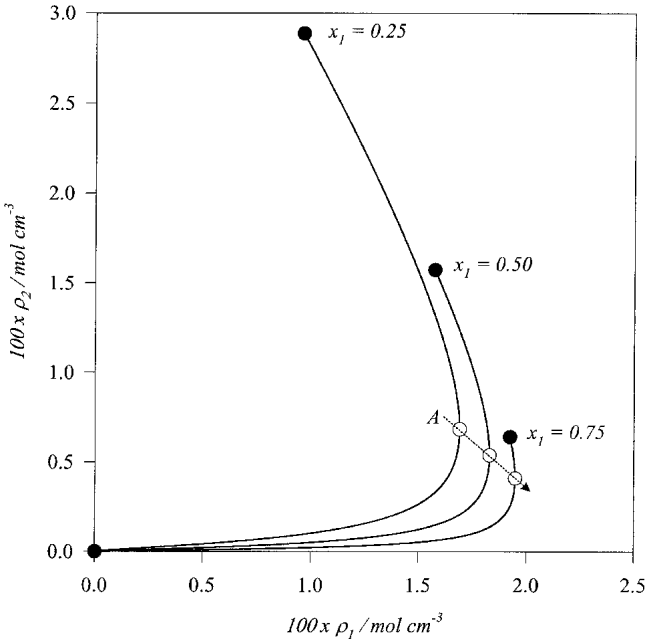

Fig. 1 ρ_1–ρ_2 projections at different mole fractions for methanol (1) + water (2) at 303.15 K. (—) GT + PR-EOS + WS + Wilson model results; (●) VLE bulk densities from PR-EOS + WS + Wilson model; (○) stationary points for water (SP_2)

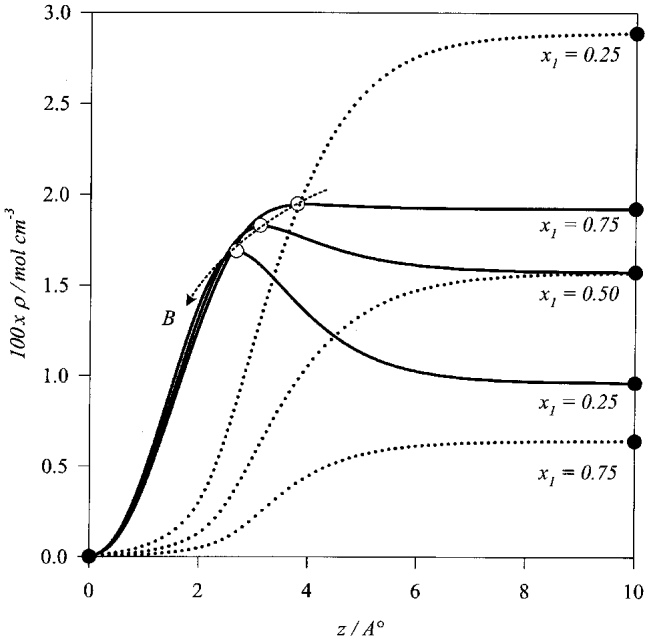

Fig. 2 z–ρ_i projections at different mole fractions for methanol (1) + water (2) at 303.15 K, calculated with GT + PR-EOS + WS + Wilson model. (—) z–ρ_1; (· · ·) z–ρ_2; (●) VLE bulk densities from PR-EOS + WS + Wilson model, (○) stationary points for methanol (SP_1)

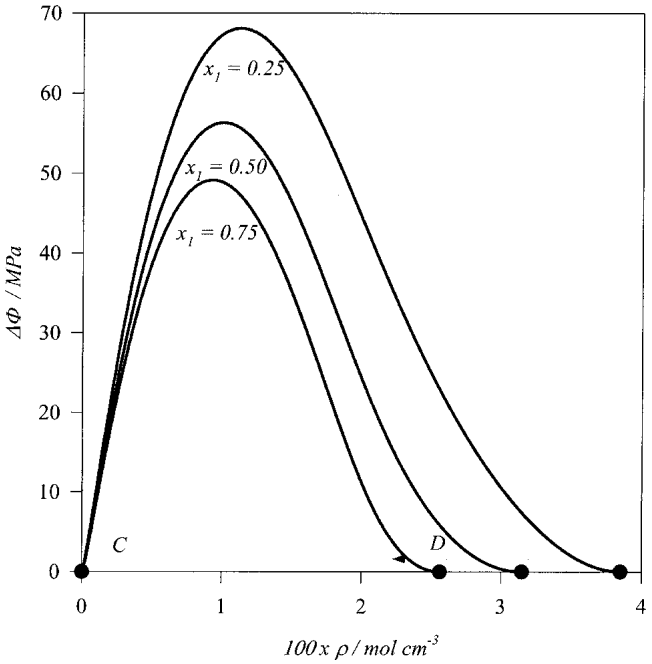

Fig. 3 ρ–ΔΦ at different mole fractions for methanol (1) + water (2) at 303.15 K. (—) Calculated from GT + PR-EOS + WS + Wilson model; (●) VLE bulk densities from PR-EOS + WS + Wilson model

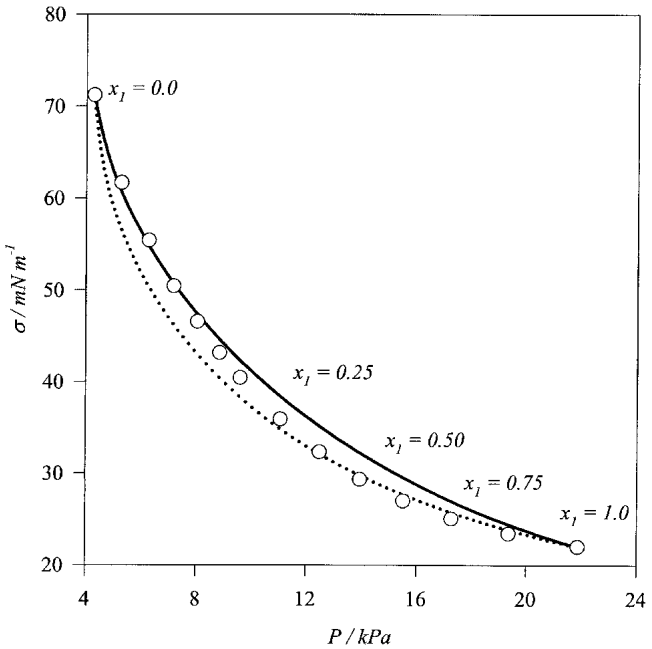

Fig. 4 *P*–σ and x_1–σ projections for methanol (1) + water (2) at 303.15 K. (· · ·) GT + PR-EOS + QMR results; (—) GT + PR-EOS + WS + Wilson results; (○) experimental σ data[38]

and x_1 increase until the azeotropic mole fraction is reached, where $[\partial\sigma/\partial P]_T = \infty$. Then σ decreases as *P* decreases and x_1 increases. This behavior is illustrated in Fig. 5 for the mixture propan-2-ol plus water.

At this point, it is important for analyzing the effect of the VLE stability on σ predictions. For the case of mixtures that contain methanol and ethanol, both the QMR and the WS models predict stable VLE. However, for mixtures that

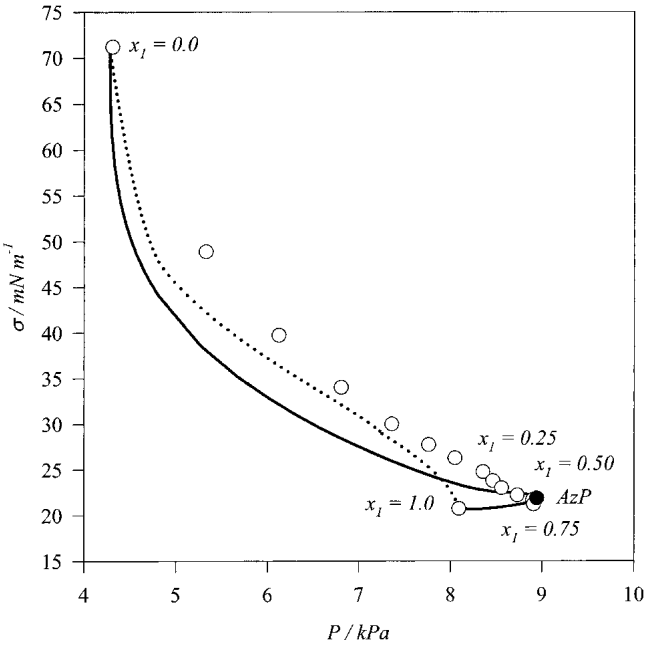

Fig. 5 P–σ and x_1–σ projections for propan-2-ol (1) + water (2) mixture at 303.15 K. (· · ·) GT + PR-EOS + QMR results; (—) GT + PR-EOS + WS + NRTL results; (●) azeotropic point (AzP); (○) experimental σ data[38]

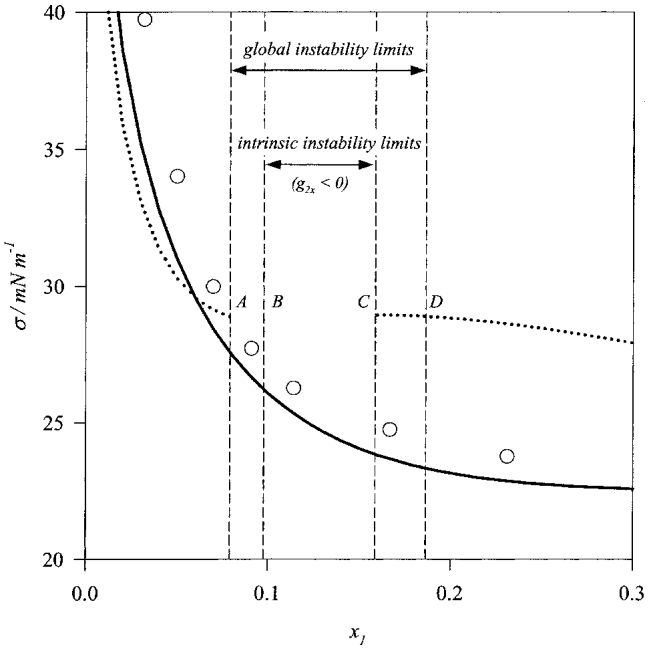

Fig. 6 x_1–σ projection for propan-2-ol (1) + water (2) at 303.15 K. (· · ·) GT + PR-EOS + QMR results; (—) GT + PR-EOS + WS + NRTL results; (---) instability limits; (○) experimental σ data[38]

contain propanol, the QMR predicts a false immiscibility gap.

Following the theory described in section 2, the concentration range in which the homogeneous liquid phase becomes unstable produces a discontinuity in σ (a nonphysical behavior, because interfaces are present in the whole concentration range). To visualize such a behavior, Fig. 6 depicts the x_1–σ projection for the mixture propan-2-ol plus water. In Fig. 6, we also included the boundaries of intrinsic and global instability, as predicted by the EOS model. In general, σ can always be calculated within the range of global stability, although never in the ranges where $g_{2x} < 0$ (range of intrinsic stability). In addition, the metastable range of a mixture does not always allow the calculation of σ. We have observed that the possibility of calculation inside metastable ranges depends on the sign of the local curvature of the vapor-pressure curve ($P_{2x} = \partial^2 P/\partial x_1^2$).

Let us fix our attention on predictions with QMR. From the results in Fig. 6, it is possible to observe that σ can be calculated from points C to D, where the mixing rule predicts that $P_{2x} > 0$. The range C to D corresponds to a metastable condition for the homogeneous liquid phase. However, for the case of the second liquid phase (rich in water), calculations can be performed only from $x_1 = 0$ to the binodal point A. No calculation inside the metastable range of the mixture (A to B) was numerically possible, and it was observed that $P_{2x} < 0$. For the mixture propan-1-ol plus water, the x_1–σ projection is similar to that in Fig. 6.

It should be pointed out that for the case of the binaries propan-2-ol and propan-1-ol plus water, no calculation of a continuous x_1–σ curve has been possible with cubic EOSs. In addition, it has been argued that the cubic EOS model with QMR is not capable of predicting σ of some polar mixtures, unless a nonzero χ_{ij} is used for averaging c_{ij} according to Eq 9.[7] Our results demonstrate that such a claim is misleading because the VLE model fails to predict the stability of the system and, consequently, the number of true phases that coexist at the equilibrium condition.

4.2 Ternary System Carbon Dioxide Plus Butane Plus Decane

In this case, we test the predictive ability of our approach for predicting σ in multicomponent mixtures. For this task, we consider binary contributions both for calculating c_{ij} and for predicting VLE. Our results for the binaries that contribute to the ternary mixture are in very good agreement with those of previous reports by other authors.[7-9,11,12,28,29] In addition, we note that no parameter in our approach has been fitted from ternary data. Figures 7 and 8 compare σ predictions with experimental values. From Fig. 7 and 8, and from Table 4 we can observe that both the QMR and original WS mixing-rules lead to better VLE predictions and result in smaller σ deviations. However, it is possible to note that both mixing-rule models underestimate the experimental data in the whole mole fraction range. This fact may be attributed to the inability of the GT and the PR-EOS appropriately describe the scaling behavior at the critical point. These results for σ are in agreement with the predictions recently reported by Miqueu et al.[12] and Miqueu[29] as can be seen in Fig. 8.

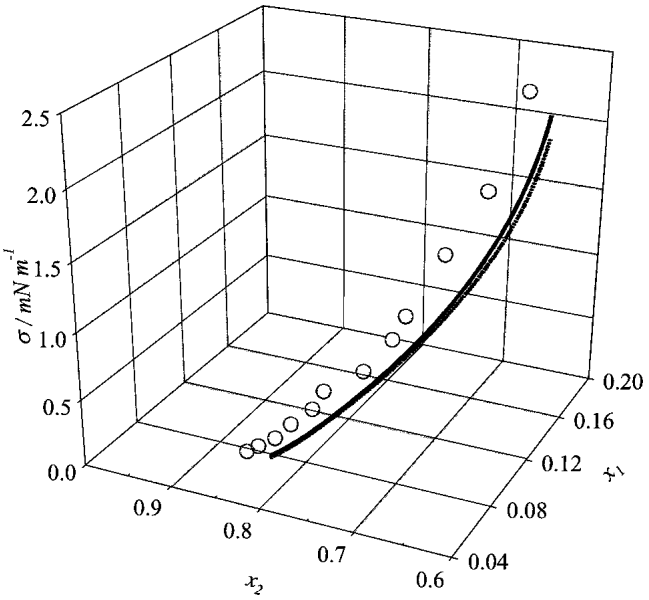

Fig. 7 x_1–x_2–σ projection for carbon dioxide (1) + butane (2) + decane (3) at 344.30 K. (· · ·) GT + PR-EOS + QMR results; (—) GT + PR-EOS + WS + NRTL results; (○) experimental σ data[39]

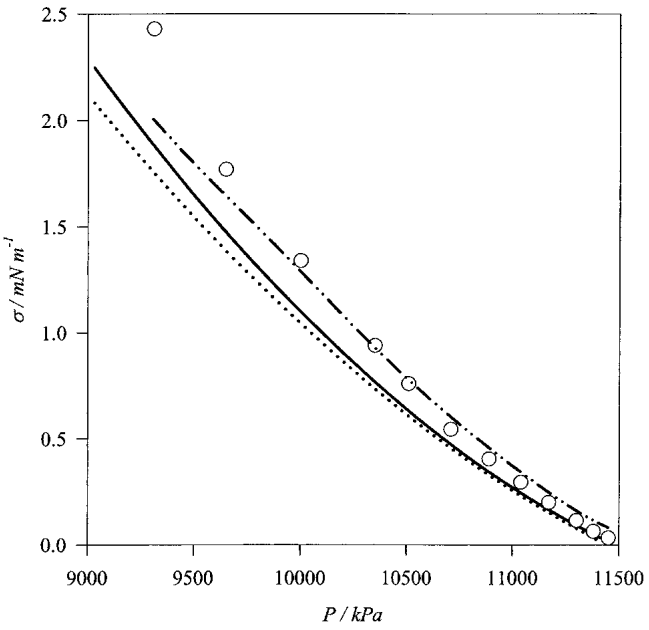

Fig. 8 *P*–σ projection for carbon dioxide (1) + butane (2) + decane (3) at 344.30 K. (· · ·) GT + PR-EOS + QMR results; (—) GT + PR-EOS + WS + NRTL results; (-··-) Miqueu et al.[12] results; (○) experimental σ data[39]

5. Concluding Remarks

In this work, we have developed an approach based on the application of the GT to a simple EOS with original WS mixing rules. Compared with traditional mixing rules, the main advantage of the original WS model is its flexibility for interpolating VLE and, then, for calculating interfacial properties under accurately predicted VLE conditions. The approach in question is useful both for correlating and for predicting interfacial tension of mixtures, and generates results that show very good agreement with the calculations of other authors.[7-9,11,12,28,29] According to our results, an adequate and accurate interpolation of VLE data allows:

- Experimental fit of σ data over the whole mole fraction range of binary mixtures;
- Reasonable prediction of the σ trend, if experimental data are not available, by assuming $\chi_{ij} = 0$; and
- A fair prediction of the σ is warranted

In addition, we demonstrated that the σ behavior is governed by the VLE, and, consequently, the analysis of the interface behavior by means of GT is constrained to mixing rules that predict an accurate and stable VLE.

Finally, from the previous results, we note that the approach of GT plus EOSs with an appropriate mixing rule produces very good predictions for mixtures of carbon dioxide plus hydrocarbons. However, for mixtures of alcohols plus water, the quoted approach needs experimental data on σ in order to obtain an adequate correlation of σs.

Acknowledgments

This work was financed by FONDECYT, Santiago, Chile (Project 2010100). Partial financing by the Israeli Science Foundation, Grant Number 340/00, is also acknowledged.

Appendix: Expressions for Homogeneous Fluids

In this work, we consider the PR-EOS and two mixing rule models (QMR and original WS) to describe the homogeneous fluid. The PR-EOS is given by[10]:

$$P = -\frac{RT\rho}{1-\rho b} - \frac{a\rho^2}{1-2\rho b+\rho^2 b^2} \qquad \text{(Eq A1)}$$

where R is the gas constant, T is temperature, P is pressure, ρ is the molar density, a is the cohesion parameter, and b is the covolume that, for the case of pure fluids, are defined as:

$$a_i = 0.457235\,\frac{(RT_{c,i})^2}{P_{c,i}}\,\alpha(T,T_{c,i}) \qquad \text{(Eq A2)}$$

$$b_i = 0.077796\,\frac{RT_{c,i}}{P_{c,i}} \qquad \text{(Eq A3)}$$

In Eq A2 and A3, $T_{c,i}$, $P_{c,i}$ are the critical temperature and pressure of pure fluids, respectively, and α_i is the thermal cohesion function:

$$\alpha_i = (1 + m_i[1 - \sqrt{T/T_{c,i}}])^2 \qquad \text{(Eq A4)}$$

where m_i, the Soave's factor, is a parameter that can be generalized in terms of the acentric factor or, as in the case of this work, may be directly fitted from vapor pressure data of pure components (see Wisniak et al.[17] for details). Equations A2 and A3 are extended to mixtures using mixing rules. When considering QMR, the cohesion parameter and the covolume of the mixture are given by the following expressions[13]:

$$a = \frac{1}{\rho^2}\sum_{i,j=1}^{n_c}\rho_i\rho_j\sqrt{a_i a_j}\,(1-k_{ij}) \qquad \text{(Eq A5)}$$

$$b = \frac{1}{\rho}\sum_{i=1}^{n_c}\rho_i b_i \qquad \text{(Eq A6)}$$

where k_{ij} is the interaction parameter, ρ_i is the concentration of component i, ρ is the concentration of the mixture. ρ and ρ_i are related by the mole fraction x_i according to $\rho_i = x_i\,\rho$. For the case of the original WS mixing rule, the parameters a and b are calculated as follows[16]:

$$a = \frac{RT\left(\sum_{i,j=1}^{n_c}\frac{\rho_i\rho_j}{\rho^2}\left[\left(b_{ii}-\frac{a_{ii}}{RT}\right)+\left(b_{jj}-\frac{a_{jj}}{RT}\right)\right]\frac{(1-k_{ij})}{2}\right)}{\left(1-\sum_{i,j=1}^{n_c}\frac{\rho_i}{\rho}\frac{a_i}{RTb_i}+\frac{G^E}{RT}\frac{\sqrt{2}}{\ln(\sqrt{2}-1)}\right)} \qquad \text{(Eq A7)}$$

$$b = \frac{\sum_{i,j=1}^{n_c}\frac{\rho_i\rho_j}{\rho_2}\left[\left(b_{ii}-\frac{a_{ii}}{RT}\right)+\left(b_{jj}-\frac{a_{jj}}{RT}\right)\right]\frac{(1-k_{ij})}{2}}{\left(1-\sum_{i,j=1}^{n_c}\frac{\rho_i}{\rho}\frac{a_i}{RTb_i}+\frac{G^E}{RT}\frac{\sqrt{2}}{\ln(\sqrt{2}-1)}\right)} \qquad \text{(Eq A8)}$$

where G^E is the excess Gibbs energy, which parametrized from an activity coefficient model. In this work, we have considered the G^E-NRTL and G^E-Wilson equations.[21]

References

1. H.T. Davis and L.E. Scriven, Gradient Theory of Fluid Microstructures, *J. Stat. Phys.,* Vol 24, 1981, p 243-268
2. J.W. Cahn and J.E. Hilliard, Free Energy of a Nonuniform System. I. Interfacial Free Energy, *J. Chem. Phys.,* Vol 28, 1958, p 258-267
3. H. Kahl and S. Enders, Calculation of Surface Properties of Pure Fluids Using Density Gradient Theory and SAFT-EOS, *Fluid Phase Equilib.,* Vol 172, 2000, p 27-42
4. P. van Konynenburg and R. Scott, Critical Lines and Phase Equilibria in Binary van der Waals Mixtures, *Philos. Trans. R. Soc. London, Ser. A,* Vol 298, 1980, p 495-539
5. B.S. Carey, "The Gradient Theory of Fluid Interfaces," Ph.D. dissertation, University of Minnesota, 1979
6. B.S. Carey, L.E. Scriven, and H.T. Davis, Semiempirical Theory of Surface Tension of Binary Systems, *AIChE J.,* Vol 26, 1980, p 705-711
7. P.M.W. Cornelisse, "The Gradient Theory Applied, Simultaneous Modelling of Interfacial Tension and Phase Behaviour," Ph.D. dissertations, Delft University, 1997
8. P.M.W. Cornelisse, C.J. Peters, and J. de Swaan Arons, Application of the Peng-Robinson Equation of State to Calculate Interfacial Tensions and Profiles at Vapor-Liquid Interfaces, *Fluid Phase Equilibr.,* Vol 82, 1993, p 119-129
9. P.M.W. Cornelisse, C.J. Peters, and J. de Swaan Arons, Simultaneous Prediction of Phase Equilibria, Interfacial Tension and Concentration Profiles, *Mol. Phys.,* Vol 80, 1993, p 941-955
10. D.Y. Peng and D.B. Robinson, A New Two-Constant Equation of State, *Ind. Eng. Chem. Fundam.,* Vol 15, 1976, p 59-64
11. M. Sahimi and B.N. Taylor, Surface Tension of Binary Liquid-Vapor Mixtures: A Comparison of Mean Field and Scaling Theories, *J. Chem. Phys.,* Vol 95, 1991, p 6749-6761
12. C. Miqueu, B. Mendiboure, C. Graciaa, and J. Lachaise, Modelling of the Surface Tension of Binary and Ternary Mixtures With the Gradient Theory of Fluid Interfaces, *Fluid Phase Equilib.,* Vol 218, 2004, p 189-203
13. H. Orbey and S.I. Sandler, *Modeling Vapor Liquid Equilibria: Cubic Equations of State and Their Mixing Rules,* Cambridge University Press, New York, 1998
14. P.M.W. Cornelisse, M. Wijtkamp, and J. de Swaan Arons, Interfacial Tensions of Fluid Mixtures With Polar and Associating Components, *Fluid Phase Equilibr.,* Vol 150/151, 1998, p 633-640
15. H. Kahl and S. Enders, Interfacial Properties of Binary Mixtures, *Phys. Chem. Chem. Phys.,* Vol 4, 2002, p 931-936
16. D. Wong and S.I. Sandler, A Theoretically Correct Mixing Rule for Cubic Equations of State, *AIChE J.,* Vol 38, 1992, p 671-680
17. J. Wisniak, A. Apelblat, and H. Segura, Application of Cubic Equations of State to the Fit of Vapor Pressure of Pure Components, *Chem. Eng. Sci.,* Vol 53, 1998, p 743-751
18. H. Van Ness and M. Abbott, *Classical Thermodynamics of Nonelectrolyte Solutions,* McGraw-Hill, New York, 1982
19. H.T. Davis and L.E. Scriven, Stress and Structure in Fluid Phase Interfaces, *Adv. Chem. Phys.,* Vol 49, 1982, p 357-454
20. H.T. Davis, *Statistical Mechanics of Phases, Interfaces, and Thin Films,* Wiley, New York, 1996
21. S.M. Walas, *Phase Equilibria in Chemical Engineering,* Butterworth, Boston, 1982
22. J.S. Rowlinson and B. Widom, *Molecular Theory of Capillarity,* Oxford University Press, Oxford, 1989
23. J. Winkelmann, The Liquid-Vapour Interface of Pure and Mixtures: Application of Computer Simulation and Density Functional Theory, *J. Phys.: Condens. Matter,* Vol 13, 2001, p 4739-4768
24. J.C. Pàmies, "Bulk and Interfacial Properties of Chain Fluids: A Molecular Modelling Approach," Ph.D. dissertation, Universitat Rovira i Virgili, 2003
25. D. Duque, J.C. Pàmies, and L.F. Vega, Interfacial Properties of Lennard-Jones Chains by Direct Simulation and Density Gradient Theory, *J. Chem. Phys.,* Vol 121, 2004, p 11,395-11,401
26. M. Modell and J. Tester, *Thermodynamics and Its Applications,* 3rd ed., Prentice Hall, New York, 1996
27. B. Widom, Structure of the $\alpha\gamma$ Interface, *J. Chem Phys.,* Vol 68, 1978, p 3878-3883
28. A. Mejía, H. Segura, L.F. Vega, and J. Wisniak, Simultaneous Prediction of Interfacial Tension and Phase Equilibria in Binary Mixtures. An Approach Based on Cubic Equations of

State With Improved Mixing Rules, *Fluid Phase Equilib.,* Vol 227, 2005, p 225-238

29. C. Miqueu, "Modélisation, à température et pression élevées, de la tension superficielle de composants des fluides pétroliers et de leurs mélanges synthétiques ou réels," Ph.D. dissertation, Université de Pau et des Pays de l'Adour, France, 2001
30. R.C. Reid, J.M. Prausnitz, and B.E. Poling, *The Properties of Gases and Liquids,* 4th ed., McGraw-Hill Book Co., Singapore, 1998
31. J.J.C. Hsu, N. Nagarajan, and R.L. Robinson Jr., Equilibrium Phase Compositions, Phase Densities, and Interfacial Tensions for Carbon Dioxide + Hydrocarbon Systems. 1. Carbon Dioxide + n-Butane, *J. Chem. Eng. Data,* Vol 30, 1985, p 485-491
32. H.H. Raemer and B.H. Sage, Phase Equilibria in Hydrocarbon Systems. Phase Behavior in the n-Butane-n-Decane System, *J. Chem. Eng. Data,* Vol 9, 1964, p 24-28
33. N. Nagarajan and R.L. Robinson Jr., Equilibrium Phase Compositions, Phase Densities, and Interfacial Tension for CO_2 + Hydrocarbon Systems. 2. CO_2 + n-Decane, *J. Chem. Eng. Data,* Vol 31, 1986, p 168-171
34. R.C. Pemberton and C.J. Mash, Thermodynamic Properties of Aqueous Non-Electrolyte Mixtures. II. Vapor Pressures and Excess Gibbs Energies for Water + Ethanol at 303.15 to 363.15 K Determined by an Accurate Static Method, *J. Chem. Thermodyn.,* Vol 10, 1978, p 867-888
35. M.L. McGlashan and A.G. Williamson, Isothermal Liquid-Vapor Equilibria for System Methanol-Water, *J. Chem. Eng. Data,* Vol 21, 1976, p 196-199
36. V.V. Udovenko and T.F. Mazanko, Liquid-Vapor Equilibrium in n-Propyl Alcohol-Water and n-Propyl Alcohol-Benzene Systems, *Izv. Vyssh. Uchebn. Zaved., Khim. Khim. Tekhnol.,* Vol 15, 1972, p 1654
37. V.V. Udovenko and T.F. Mazanko, Saturated Vapor Pressures in the Isopropyl Alcohol-Benzene-Water System, *Zh. Fiz. Khim.,* Vol 41, 1967, p 1615
38. G. Vázquez, E. Alvarez, and J. Navaza, Surface Tension of Alcohol + Water from 20 to 50 °C, *J. Chem. Eng. Data,* Vol 40, 1995, p 611-614
39. N. Nagarajan, K.A.M. Gasem, and R.L. Robinson Jr., Equilibrium Phase Compositions, Phase Densities, and Interfacial Tension for CO_2 + Hydrocarbon Systems. 6. CO_2 + n-Butane + n-Decane, *J. Chem. Eng. Data,* Vol 35, 1990, p 228-231